

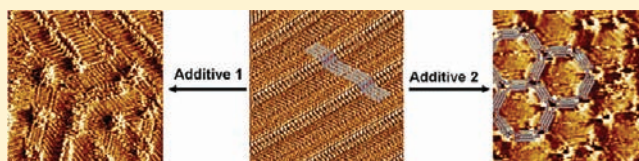
Additive Perturbed Molecular Assembly in Two-Dimensional Crystals: Differentiating Kinetic and Thermodynamic Pathways

Seokhoon Ahn and Adam J. Matzger*

Department of Chemistry and the Macromolecular Science and Engineering Program, University of Michigan, Ann Arbor, Michigan 48109-1055, United States

S Supporting Information

ABSTRACT: During attempts to produce novel two-dimensional cocrystals by coadsorbing components in a binary mixture, the formation of a metastable form was observed in analogy to the phenomenon of additive-induced polymorph formation reported in three-dimensional crystallization. Mechanistic insights into this phenomenon were gained through the use of scanning tunneling microscopy and several adsorbate/additive combinations. One additive plays a critical role in forming a disordered assembly through a process that is primarily kinetic whereas another additive thermodynamically stabilized an intermediate form, resulting in interrupting a phase transformation to a more stable form. These additive effects elucidate one of the potential pathways to kinetically isolate a metastable polymorph formed during cocrystallization in three-dimensional crystallization.



INTRODUCTION

Crystal polymorphism, because of its importance across a wide range of fields in solid-state chemistry such as pharmaceuticals,^{1,2} explosives,^{3,4} and nonlinear optical materials,^{5,6} is of considerable economic interest; furthermore, because of the unresolved challenges associated with predicting the occurrence of this phenomenon and experimentally producing forms, it is one of the most significant unresolved issues in solid state chemistry. In general, polymorphs are discovered through crystallization by screening methods varying solvent and temperature⁷ although more modern discovery methods such as tailor-made additives,^{8–10} epitaxial crystal growth,^{11–13} and polymer-induced heteronucleation¹⁴ are entering the toolbox of the solid-state researcher. Recently, the discovery of new single component crystalline polymorphs during attempts to grow cocrystals has been reported,^{15–19} and this phenomenon may be distinguished from previous methods of polymorph discovery. For example, an impressive four polymorphs of pure benzidine were obtained from attempted cocrystallizations with benzophenone and diphenyl sulfoxide.¹⁶ The generation of metastable polymorphs during cocrystallization trials may prove to be a useful crystal form discovery technique contributing to the important goal of accessing all energetically viable polymorphs of a given compound; however, at the present time, the mechanism of form production is unclear, making the path toward further developments uncertain. Because reduced dimensionality dramatically simplifies crystallization phenomena, studying phase selection in two-dimensional (2D) crystallization at solution/solid interfaces can provide mechanistic insights at the molecular level. Here we demonstrate that phase selection arises in attempted coadsorption of several additives with a simple amide amphiphile capable of forming multiple phases. These results were obtained by scanning tunneling microscopy (STM), offering submolecular resolution of both periodic and nonperiodic packing in a time dependent

fashion,^{20–28} and the results are interpreted in the context of kinetics and thermodynamics.

RESULTS AND DISCUSSION

To explore the effect of additives on phase selection in 2D crystals, an amide amphiphile with 18 carbons in the alkyl chain (**18-amide**) was selected for study because it has been shown to form at least six phases.²⁹ The chemical structure of **18-amide** and the additive molecules investigated are shown in Figure 1. A concentration of 100 μM total adsorbate was used for each binary mixture with the molar ratio varied as specified. All STM imaging was performed at the phenyloctane/highly oriented pyrolytic graphite (HOPG) interface. During this investigation, new crystallization behaviors, distinguished from those occurring in the homogeneous solutions of **18-amide**, were observed and in some cases the results are kinetic in nature whereas for others the presence of an additive exerts a thermodynamic influence. The implications of these results for understanding additive effects on three-dimensional (3D) polymorph selection are discussed in this context.

18-Amide with 17-*m*-Diester. As a baseline for understanding additive effects, the case of **18-amide** with **17-*m*-diester** is discussed. At high concentrations of the amide, a pure close packed phase (Figure 2, phase I) is observed. A rhombic nanoporous network of **18-amide** (Figure 2, phase II) was observed from 1:3 to 1:11 (**18-amide**:**17-*m*-diester**) whereas coadsorption occurred from 1:11 to 1:20 to form 1D-cocrystals.²⁸ These molecular assemblies showed a marked dependence on the relative mole fraction of two components in solution. The structural characteristics of these phases have been discussed previously.^{28–30} In particular, coexistence of

Received: November 21, 2011

Published: February 6, 2012

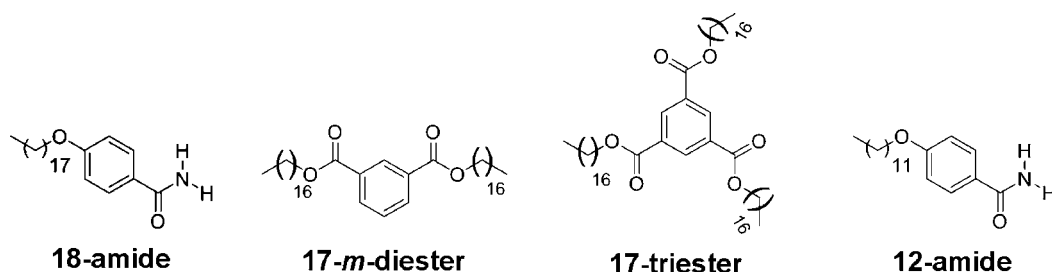


Figure 1. Chemical structures of the molecules investigated.

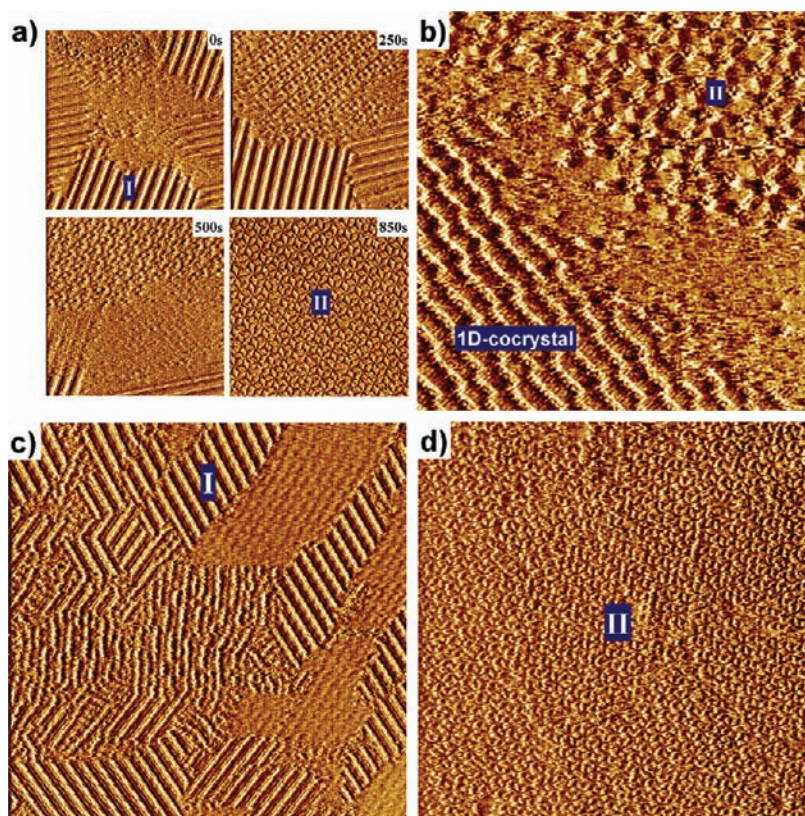


Figure 2. Assemblies obtained from the competition study of **18-amide** and **17-m-diester**. Blue insets identify phases. (a) STM images ($100 \times 100 \text{ nm}^2$) showing phase transformation from the close packed phase (phase I) to the rhombic nanoporous network (phase II) observed at 1:6 (**18-amide**/**17-m-diester**). (b) STM image ($50 \times 50 \text{ nm}^2$) showing coadsorption of phase II of **18-amide** and 1D-cocrystal at a 1:11 ratio. (c) STM image ($200 \times 200 \text{ nm}^2$) obtained from 1:9 ratio with $52 \mu\text{M}$ **18-amide**. (d) STM image ($200 \times 200 \text{ nm}^2$) obtained from 1:9 ratio with $10 \mu\text{M}$ **18-amide**.

phase II of **18-amide** and the 1D-cocrystal without phase transformation was observed at 1:11 (Figure 2b), indicating that competitive adsorption occurs near this molar ratio so that the formation of phase II of **18-amide** may be influenced by molecular interaction with **17-m-diester**. However, the above data are also consistent with a simple dilution effect in a single or multicomponent solution,^{24,29,31–34} which has been shown to stabilize phase II in a homogeneous **18-amide** solution.²⁹ To test this hypothesis, the concentration of **18-amide** in the mixture was varied while keeping the molar ratio to the additive constant. Using $53 \mu\text{M}$ **18-amide** and $460 \mu\text{M}$ **17-m-diester** (1:9), the concentration of **18-amide** is above the stability crossing point between phase I and II observed in homogeneous solution ($33 \mu\text{M}$).²⁹ Under these conditions, phase II was not observed and some disorder, which may be kinetically induced by competition, was observed (Figure 2c). However, at $10 \mu\text{M}$ **18-amide** and $90 \mu\text{M}$ **17-m-diester** (1:9),

phase II was observed as the thermodynamically stable form (Figure 2d). This competition study with **17-m-diester** does not illuminate new thermodynamic behavior based on the presence of an additive although competitive adsorption exerts some influence on kinetics of nucleation and aggregate formation as evidenced by the formation of disorder. This kinetic effect exerted by an additive was also observed in the competition with **17-triester** as discussed below.

18-Amide with 17-Triester. A highly disordered assembly of **18-amide** domains was observed from 2:1 (**18-amide**/**17-triester**) without discernible **17-triester** coadsorption (Figure 3a) whereas coadsorption with phase segregation between the disordered assembly of **18-amide** and pure **17-triester** was observed at a 1:1 ratio (Figure 3b). Because a disordered structure has not been observed in dilute solutions of **18-amide**,²⁹ amide amphiphile analogues with shorter alkyl chains,³⁰ nor in the mixture with other additives in the present

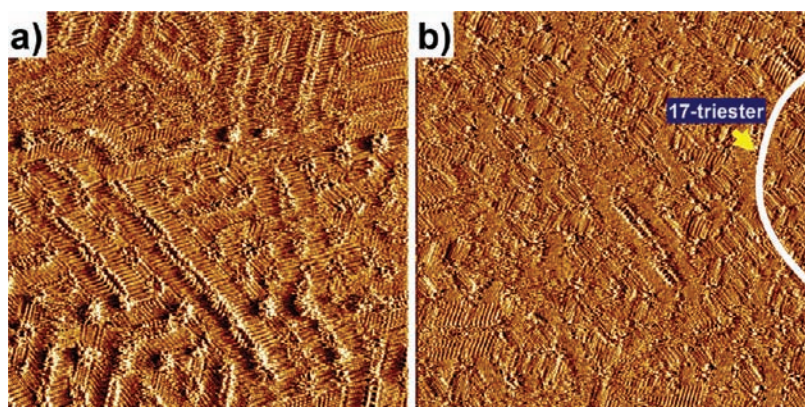


Figure 3. Assemblies obtained from the competition study of **18-amide** and **17-triester**. (a) STM image ($50 \times 50 \text{ nm}^2$) of the disordered structure of **18-amide** initially observed at 2:1 (**18-amide**/**17-triester**). (b) STM image ($50 \times 50 \text{ nm}^2$) showing coadsorption of **18-amide** and **17-triester** at a 1:1 ratio.

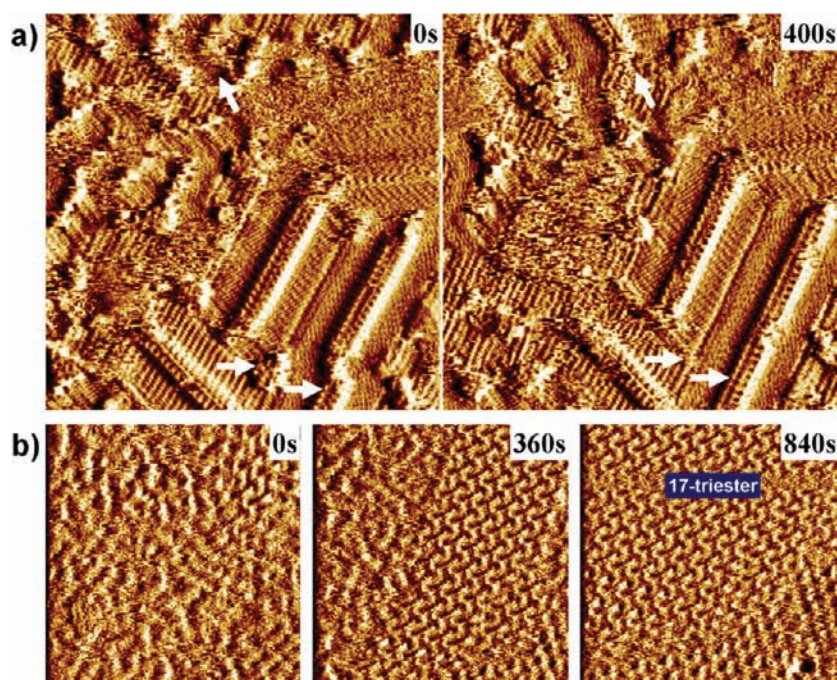


Figure 4. Time course observation of assemblies indicating that the disordered phase of **18-amide** is a kinetic product induced by the competition with **18-amide** and **17-triester**. (a) STM images ($25 \times 25 \text{ nm}^2$) obtained at 2:1 (**18-amide**/**17-triester**) showing conversion to the more ordered structure. (b) STM images ($50 \times 50 \text{ nm}^2$) showing the transformation from a disordered **18-amide** phase to the ordered **17-triester** phase at a 1:1 ratio.

study, the disordered assembly is believed to be induced from molecular interaction between **18-amide** and **17-triester** and furthermore is a kinetic product. This latter claim is supported by the observation of the transformation from disordered to ordered structures during sequential STM images (Figure 4). The disordered structure observed at a 1:1 ratio reorganizes to form more ordered structures indicated by white arrows in Figure 4a, a type of Ostwald ripening (see Supporting Information).^{35–39} With further increase of the **17-triester** fraction, the disordered structures of **18-amide** are replaced by **17-triester** phase (Figure 4b). In this case, the dilution is unlikely to significantly affect crystallization because the concentration of **18-amide** in the present case is greater than the $33 \mu\text{M}$ stability crossover point between phase I and II in homogeneous solution; therefore the displacement reflects a competition for limited adsorption sites with the most strongly adsorbed molecule covering the surface. In a previous study it was

demonstrated that **18-amide** has the ability to form and stabilize various aggregates through noncovalent interactions and when two different aggregates are incorporated in a unit cell, highly complex features such as one-dimensional order and wave-like patterns of voids are formed.²⁹ The same phenomenon manifests in the present case because the existence of various aggregates in the disordered assembly is observed while maintaining reasonably close packing due to compatibility of aggregates. In other words this compatibility between various aggregates makes disorder possible to observe because the thermodynamic penalty is not great.

18-Amide with 12-Amide. During 2D crystal growth of **18-amide** in the presence of **12-amide**, the formation of the honeycomb network (phase III) and the rhombic nanoporous networks (phase II) of **18-amide** were observed at ratios from 1:3 to 1:7 (**18-amide**/**12-amide**) (Figure 5) whereas the

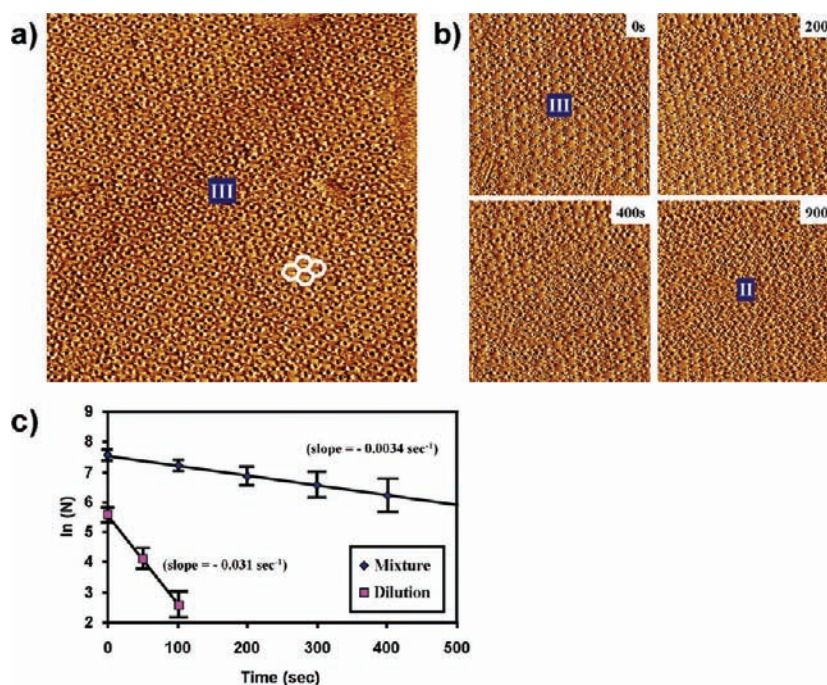


Figure 5. Assemblies obtained from the competition study of **18-amide** and **12-amide**. (a) STM image ($200 \times 200 \text{ nm}^2$) of the honeycomb nanoporous network (phase III) with 95% surface coverage at 1:3 (**18-amide/12-amide**). (b) STM images ($100 \times 100 \text{ nm}^2$) showing phase transformation from phase III to II observed at 1:3. (c) Plots regarding phase transformation from phase III to II observed from the mixture and the diluted homogeneous solution of $25 \mu\text{M}$ of **18-amide** at room temperature. N is the number of molecules counted.

rhombic nanoporous network of **12-amide** was observed at a ratio of 1:9. The formation of any bilayer was not observed under different STM bias voltages. The present case differs from 2D crystallization from **18-amide** homogeneous solutions in two ways: (1) The phase III of **18-amide** obtained in the presence of additive was observed as a major phase with over 95% surface coverage whereas the surface coverage by phase III in homogeneous solutions was less than 10%,²⁵ and (2) the phase transformation rate from phase III to II dramatically decreased in the two component system compared with that observed in homogeneous solutions. The phase transformation rate was obtained by counting the number of molecules (N) associated with each phase in successive STM images. To eliminate concentration effects on the rate, the concentration of **18-amide** for both the mixture and the homogeneous solution were fixed at $25 \mu\text{M}$. Because the phase transformation occurred most rapidly in the scanned area, the scanning parameters such as current, bias, and scanning rate were fixed and the average of the rates obtained by STM imaging with different tips was used to minimize tip artifacts. The obtained values of $\ln(N)/\text{sec}$ were -0.031 ± 0.007 for the diluted homogeneous solution and -0.0034 ± 0.0012 for the mixture (Figure 5c). This 10-fold difference is consistent with an increase in activation energy required to transform from phase III to II in the presence of the additive. Using the Arrhenius equation, the change of the energy barrier (ΔE_a) associated with this transformation can be estimated as $1.33 \pm 0.36 \text{ kcal/mol}$ (see Supporting Information).^{40,41} This increase of energy barrier (E_a) can be achieved by either destabilization of the transition state between phase III and II (kinetic mechanism) or stabilization of phase III (thermodynamic mechanism). Although kinetic factors often explain the formation of a metastable form during crystallization with additives in 3D crystallization, the thermodynamic stabilization of a metastable

form is generally not possible in 3D crystallization because in a pure phase additive can only interact with the surface of the crystals and this exerts a negligible effect on stability. The differentiation between these possibilities in 2D could be achieved by comparing STM images obtained during the phase transformation in homogeneous solution and the mixture (Figure 6). In the homogeneous solution of $25 \mu\text{M}$ **18-amide**, because phase III is kinetically formed after desorption of a part of phase I and rapidly transformed to phase II, phase I and II exist as major phases as shown in Figure 6a. In contrast, phase I was rarely observed in the mixture of **18-amide** and **12-amide** as shown in Figure 6c whereas phase III exists as a major phase. This observation can not be explained by the kinetic pathway. In that case phase I should be observed as one of the major phases because phase I remains more stable than phase III. However, the observed phenomenon suggests that phase III is more stable than phase I. To verify this thermodynamic stabilization pathway, $0.5 \mu\text{L}$ of $100 \mu\text{M}$ of **18-amide** was placed on HOPG. After confirming the formation of phase I by STM, $1.5 \mu\text{L}$ of $100 \mu\text{M}$ **12-amide** was added to the solution on HOPG to make a 1:3 mixture that is $25 \mu\text{M}$ in **18-amide**. The phase transformation from phase I to III occurred as shown in Figure 7. This result indicates that phase III is more stable than phase I under these conditions, a result of combining dilution effects and a thermodynamic stabilization of phase III by **12-amide** molecules. Thermodynamic stabilization of a nanoporous network in 2D crystallization of a single component solution can occur by three general pathways:^{29,31,32} (1) epitaxial stabilization by due to substrate, (2) equilibrium of adsorption–desorption (dilution), and (3) solvent coadsorption. The constancy of the substrate and concentration employed points to the role of **12-amide** molecules as stabilizers of phase III through a coadsorption mechanism analogous to (3). A closely related phenomenon is cocrystallization through host–guest chemistry. For example, the

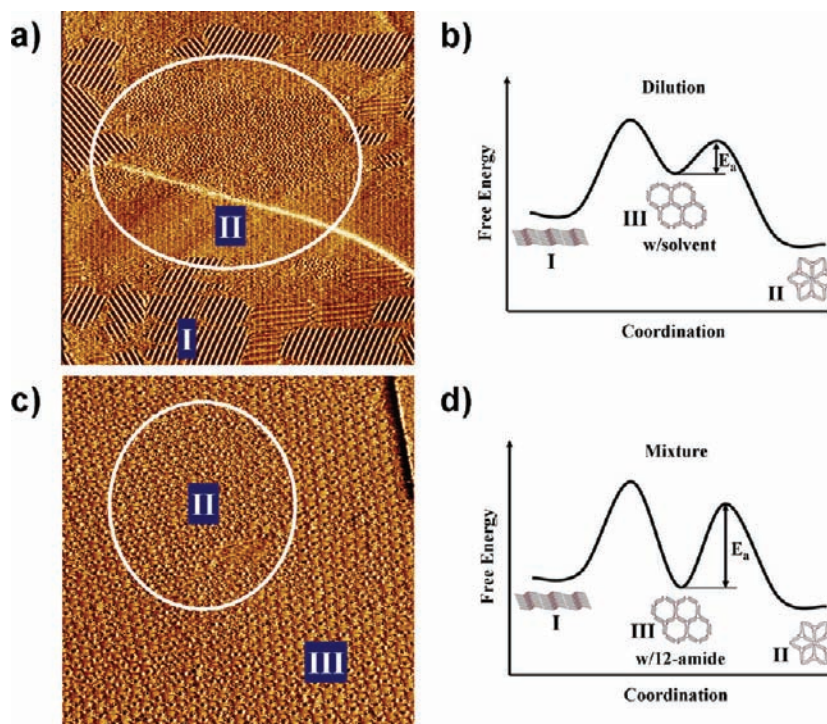


Figure 6. STM images ((a) $400 \times 400 \text{ nm}^2$, (c) $200 \times 200 \text{ nm}^2$) and reaction coordinate diagram of the phase transformation from (a, b) the homogeneous solution of $25 \mu\text{M}$ and (c, d) the mixture of 1:3 (18-amide/12-amide) with $25 \mu\text{M}$ of 18-amide. In the 18-amide homogeneous solutions, phase III is observed as a kinetic intermediate at the boundary area between phase I and II. However, in the mixture with 12-amide, phase III is observed as a major phase and slowly transformed to phase II where phase I was rarely observed, indicating that phase III can be more stable than phase I in the mixture.

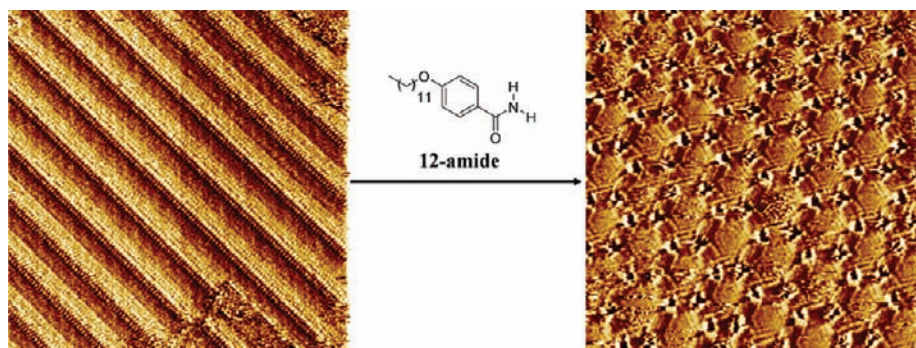


Figure 7. STM images ($50 \times 50 \text{ nm}^2$) showing the role of 12-amide molecules as stabilizers of phase III. Phase I formed from the homogeneous solution was transformed to phase III by adding 12-amide solution to make a 1:3 mixture (18-amide/12-amide).

linear structure of dehydrobenzo[12]annulene derivatives were transformed to the honeycomb structure by adding excess coronene molecules that fill empty space.⁴² The failure to image coadsorbed 12-amide molecules in the present case must be related to their high mobility. Therefore, the high surface coverage of phase III and the transformation rate decrease from phase III to II in the mixture can only be rationalized by the thermodynamic stabilization of phase III by 12-amide molecules.

Implications. The above three cases illustrate that an additive can kinetically and/or thermodynamically affect the 2D crystallization of 18-amide (Figure 8). From these competition studies, three major factors in 2D phase selection from multicomponent solutions were identified. First, the mole fraction of components plays a critical role, in concert with the free energy of monolayer formation, in determining which phase adsorbs at equilibrium (see Supporting Information for the monolayer formation dependence

on mole fraction in the present cases). Second, dilution effects serve as a key thermodynamic factor in 2D crystallization. Third, additive structures play a critical role in determining 2D crystal structure through a kinetic and/or thermodynamic mechanism. In particular, assembly structure as well as stabilization of a metastable form can be controlled through modification of additive structure.

The above 2D phenomena involving competitive molecular adsorption offers a mechanism to explain changes in the course of phase selection from multicomponent solutions in 3D crystallization. Heterogeneous nucleation is a ubiquitous phenomenon in 3D crystallization and therefore the structure of adlayers, such as physisorbed monolayers examined here, may kinetically drive the outcome of crystallization. The above examples illustrate that monolayer structure can be altered, in a dynamic fashion, both through kinetic and thermodynamic pathways; inasmuch as such structures can exert kinetic

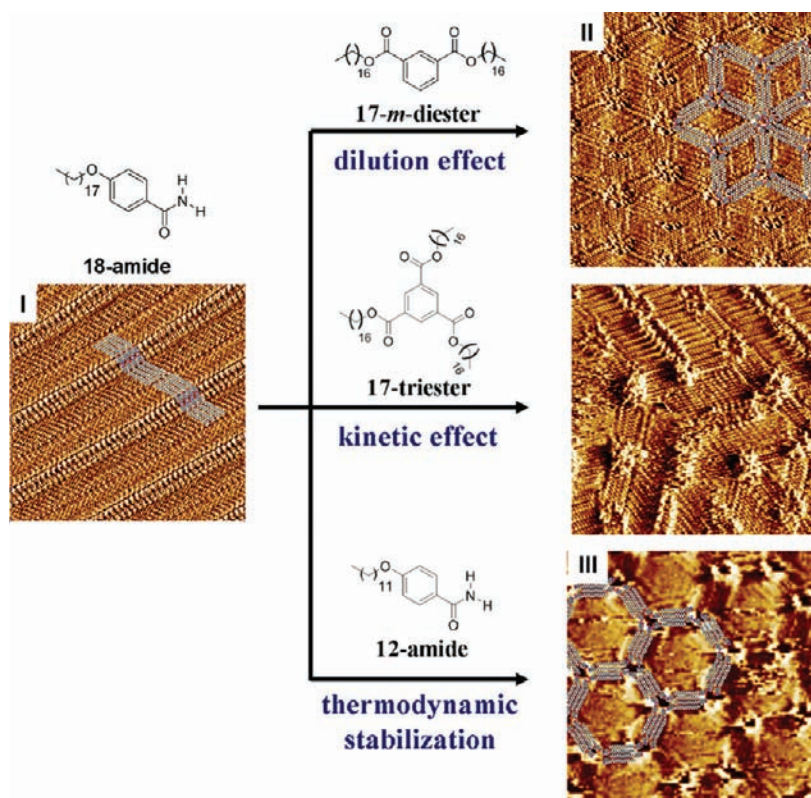


Figure 8. Overview of the competition study with an additive. The molar ratio, concentration effect, and an additive structure play a critical role in determining the assembly of 18-amide.

influence over phase selection in 3D crystallization through a heteronucleation mechanism this offers one pathway for additive-induced polymorph selection/discovery in 3D crystallization.

CONCLUSION

The phenomenon of additive-induced phase selection reported in 3D crystallization has close analogy in 2D crystallization. The reduced dimensionality and ability to probe the 2D system by STM allows mechanistic insights into this phenomenon at the molecular level. The molecular interaction between two components plays a critical role in determining assembly structure through kinetic and thermodynamic mechanisms and each plays a role that is dependent on the details of monolayer structure. Because these observations in 2D crystallization can be applied to heteronucleation occurring during attempted cocrystallization, the influence of an additive on adlayer formation may be one of the operative pathways to kinetically produce a metastable polymorph. In other words, although thermodynamic stabilization of a metastable form by an additive is without analogy in 3D crystallization of polymorphs, the thermodynamic selection of 2D crystal forms does offer a potential explanation for kinetic control of polymorphism in cases where heteronucleation prevails.

ASSOCIATED CONTENT

Supporting Information

Synthesis of 17-triester, experimental details, molar ratio dependent phase change, additional STM images, and determination of the difference of activation energy. This

material is available free of charge via the Internet at <http://pubs.acs.org>.

AUTHOR INFORMATION

Corresponding Author

*matzger@umich.edu

ACKNOWLEDGMENTS

This work was supported by the National Science Foundation (CHE-0957591).

REFERENCES

- (1) López-Mejías, V.; Kampf, J. W.; Matzger, A. J. *J. Am. Chem. Soc.* **2009**, *131*, 4554–4555.
- (2) Vishweshwar, P.; McMahon, J. A.; Oliveira, M.; Peterson, M. L.; Zaworotko, M. J. *J. Am. Chem. Soc.* **2005**, *127*, 16802–16803.
- (3) Vrcelj, R. M.; Sherwood, J. N.; Kennedy, A. R.; Gallagher, H. G.; Gelbrich, T. *Cryst. Growth Des.* **2003**, *3*, 1027–1032.
- (4) van der Heijden, A.; Bouma, R. H. B. *Cryst. Growth Des.* **2004**, *4*, 999–1007.
- (5) Nalwa, H. S.; Saito, T.; Kakuta, A.; Iwayanagi, T. *J. Phys. Chem.* **1993**, *97*, 10515–10517.
- (6) Kwon, O. P.; Jazbinsek, M.; Yun, H.; Seo, J. I.; Kim, E. M.; Lee, Y. S.; Gunter, P. *Cryst. Growth Des.* **2008**, *8*, 4021–4025.
- (7) Rodríguez-Spong, B.; Price, C. P.; Jayasankar, A.; Matzger, A. J.; Rodríguez-Hornedo, N. *Adv. Drug Delivery Rev.* **2004**, *56*, 241–274.
- (8) Weissbuch, I.; Addadi, L.; Lahav, M.; Leiserowitz, L. *Science* **1991**, *253*, 637–645.
- (9) Thallapally, P. K.; Jetti, R. K. R.; Katz, A. K.; Carrell, H. L.; Singh, K.; Lahiri, K.; Kotha, S.; Boese, R.; Desiraju, G. R. *Angew. Chem., Int. Ed.* **2004**, *43*, 1149–1155.

- (10) He, X. R.; Stowell, J. G.; Morris, K. R.; Pfeiffer, R. R.; Li, H.; Stahly, G. P.; Byrn, S. R. *Cryst. Growth Des.* **2001**, *1*, 305–312.
- (11) Mitchell, C. A.; Yu, L.; Ward, M. D. *J. Am. Chem. Soc.* **2001**, *123*, 10830–10839.
- (12) Hiremath, R.; Basile, J. A.; Varney, S. W.; Swift, J. A. *J. Am. Chem. Soc.* **2005**, *127*, 18321–18327.
- (13) Hiremath, R.; Varney, S. W.; Swift, J. A. *Chem. Commun.* **2004**, *40*, 2676–2677.
- (14) Price, C. P.; Grzesiak, A. L.; Matzger, A. J. *J. Am. Chem. Soc.* **2005**, *127*, 5512–5517.
- (15) Ahn, S.; Guo, F.; Kariuki, B. M.; Harris, K. D. *J. Am. Chem. Soc.* **2006**, *128*, 8441–8452.
- (16) Rafilovich, M.; Bernstein, J. *J. Am. Chem. Soc.* **2006**, *128*, 12185–12191.
- (17) Roy, S.; Goud, N. R.; Babu, N. J.; Iqbal, J.; Kruthiventi, A. K.; Nangia, A. *Cryst. Growth Des.* **2008**, *8*, 4343–4346.
- (18) Day, G. M.; Trask, A. V.; Motherwell, W. D. S.; Jones, W. *Chem. Commun.* **2006**, 54–56.
- (19) Aakeröy, C. B.; Desper, J.; Levin, B. *Acta Cryst. C* **2005**, *61*, o702–o704.
- (20) Lei, S.; Tahara, K.; Adisoejoso, J.; Balandina, T.; Tobe, Y.; De feyter, S. *CrystEngComm* **2010**, *12*, 3369–3381.
- (21) Scherer, L. J.; Merz, L.; Constable, E. C.; Housecroft, C. E.; Neuburger, M.; Hermann, B. A. *J. Am. Chem. Soc.* **2005**, *127*, 4033–4041.
- (22) Fang, H. B.; Giancarlo, L. C.; Flynn, G. W. *J. Phys. Chem. B* **1999**, *103*, 5712–5715.
- (23) He, Y.; Ye, T.; Borguet, E. *J. Phys. Chem. B* **2002**, *106*, 11264–11271.
- (24) Kampschulte, L.; Werblowsky, T. L.; Kishore, R. S. K.; Schmittl, M.; Heckl, W. M.; Lackinger, M. *J. Am. Chem. Soc.* **2008**, *130*, 8502–8507.
- (25) Wei, Y. H.; Kannappan, K.; Flynn, G. W.; Zimmt, M. B. *J. Am. Chem. Soc.* **2004**, *126*, 5318–5322.
- (26) Tao, F.; Bernasek, S. L. *J. Phys. Chem. B* **2005**, *109*, 6233–6238.
- (27) Lackinger, M.; Heckl, W. M. *Langmuir* **2009**, *25*, 11307–11321.
- (28) Ahn, S.; Matzger, A. J. *J. Am. Chem. Soc.* **2009**, *131*, 13826–13832.
- (29) Ahn, S.; Matzger, A. J. *J. Am. Chem. Soc.* **2010**, *132*, 11364–11371.
- (30) Ahn, S.; Morrison, C. N.; Matzger, A. J. *J. Am. Chem. Soc.* **2009**, *131*, 7946–7947.
- (31) Lei, S. B.; Tahara, K.; De Schryver, F. C.; Van der Auweraer, M.; Tobe, Y.; De Feyter, S. *Angew. Chem., Int. Ed.* **2008**, *47*, 2964–2968.
- (32) Tahara, K.; Okuhata, S.; Adisoejoso, J.; Lei, S.; Fujita, T.; De Feyter, S.; Tobe, Y. *J. Am. Chem. Soc.* **2009**, *131*, 17583–17590.
- (33) Tahara, K.; Lei, S.; Mossinger, D.; Kozuma, H.; Inukai, K.; Van der Auweraer, M.; De Schryver, F. C.; Hoger, S.; Tobe, Y.; De Feyter, S. *Chem. Commun.* **2008**, *44*, 3897–3899.
- (34) Lei, S.; Tahara, K.; Tobe, Y.; De Feyter, S. *Chem. Commun.* **2010**, *46*, 9125–9127.
- (35) Florio, G. M.; Klare, J. E.; Pasamba, M. O.; Werblowsky, T. L.; Hyers, M.; Berne, B. J.; Hybertsen, M. S.; Nuckolls, C.; Flynn, G. W. *Langmuir* **2006**, *22*, 10003–10008.
- (36) De Feyter, S.; De Schryver, F. C. *J. Phys. Chem. B* **2005**, *109*, 4290–4302.
- (37) Kim, K.; Plass, K. E.; Matzger, A. J. *Langmuir* **2003**, *19*, 7149–7152.
- (38) Lackinger, M.; Griessl, S.; Kampschulte, L.; Jamitzky, F.; Heckl, W. M. *Small* **2005**, *1*, 532–539.
- (39) Stabel, A.; Heinz, R.; De Schryver, F. C.; Rabe, J. P. *J. Phys. Chem.* **1995**, *99*, 505–507.
- (40) Brown, D. E.; Moffatt, D. J.; Wolkow, R. A. *Science* **1998**, *279*, 542–544.
- (41) Lu, X.; Polanyi, J. C.; Yang, J. *Nano Lett.* **2006**, *6*, 809–814.
- (42) Furukawa, S.; Tahara, K.; De Schryver, F. C.; Van der Auweraer, M.; Tobe, Y.; De Feyter, S. *Angew. Chem., Int. Ed.* **2007**, *46*, 2831–2834.